

Malicious Corruption-Resilient Wide-Area Oscillation Monitoring using Principal Component Pursuit

Kaveri Mahapatra, *Student Member, IEEE*, and Nilanjan Ray Chaudhuri, *Senior Member, IEEE*

Abstract—A Principal Component Pursuit (PCP)-based interface is proposed between raw synchrophasor data and the algorithms used for wide-area monitoring application to provide resilience against malicious data corruption. The PCP method-based preprocessor recovers a low rank matrix from the data matrix despite gross sparse errors originating from cyber-attacks by solving a convex program. The low-rank matrix consists of the basis vectors obtained from the system response and the sparse matrix represents corruption in each position of the data matrix. An augmented Lagrangian multiplier (ALM)-based algorithm is applied to solve the PCP problem. The low rank matrix obtained after solving PCP represents the reconstructed data and can be used for estimation of poorly-damped modes. A recursive oscillation monitoring algorithm is tested to validate the effectiveness of the proposed approach under both ambient and transient conditions.

Index Terms—PCA, Principal Component Pursuit, Cyber Attack, Bad data, Wide Area Monitoring

NOMENCLATURE

[M] Raw PMU measurements of ' n_1 ' signals with ' n_2 ' samples in a ' $n_1 \times n_2$ ' matrix.

[L] Recovered PMU measurements of ' n_1 ' signals with ' n_2 ' samples in a ' $n_1 \times n_2$ ' matrix.

[S] Estimated corruption present in PMU measurements at the corresponding positions in a ' $n_1 \times n_2$ ' matrix.

U, Σ, V Matrices containing left singular vectors, singular values, and right singular vectors, respectively obtained from Singular Value Decomposition.

m Number of nonzero elements in the matrix S .

λ A positive regularization parameter used in the objective function of PCP.

σ_i i^{th} singular value of the matrix L .

u_i, v_i i^{th} left and right singular vectors associated with i^{th} singular value obtained after applying SVD on the matrix L .

$\mu(U)$ Coherence parameter of a matrix U .

P_U Orthogonal projection onto the subspace U .

e_i i^{th} Canonical basis vector.

T_W Window size of the data matrix, M .

T_{PCP} CPU time for processing PCP algorithm.

I. INTRODUCTION

Phasor Measurement Units (PMUs) play a major role in wide-area monitoring and control applications [1]–[5]. Broadly, wide-area monitoring applications can be divided into two categories [6]:

- applications requiring a full observability of the network
 - e.g. voltage instability assessment of meshed networks.
- applications not requiring an entire network observation
 - e.g. oscillation monitoring and stability assessment.

The first type of application requires state estimation (SE) using PMU data. In this paper, our focus is on the second type of application.

Notably, the second type of application of PMU data streams from Wide-Area Measurement Systems (WAMS) is already operational in control centers of many utilities including California ISO, PG&E, BPA [7], and TVA [8], and a corresponding web-based version is deployed in 7 operations centers and 11 reliability coordinators in the Eastern Interconnection [7] for quite some time. In this application, time-synchronized PMU data is communicated to a control center and the data samples are aligned by Phasor Data Concentrator, which in turn is processed by oscillation monitoring algorithms (or so-called ‘Mode Meters’ [7]–[10]) to predict modal frequency and damping. Accurate knowledge of modal frequency and damping ratio is important since they are vital indicators of system stress and stability [7], [8], [11]. Naturally, errors or corruption in PMU data will affect the accuracy of these estimations. Errors in PMU measurement are direct consequences of limited measurement precision, telecommunication equipment noise, two-way communication systems [12], interference from devices, and cyber-attacks such as eavesdropping, GPS spoofing, and data tampering [13].

A significant amount of work has been reported in literature on bad data or cyber intrusion detection pertaining to state estimation [14]–[28]. Literature on detection of bad data originated by cyber-attacks in PMU dynamic data samples include a common path algorithm [29], a hybrid intrusion detection system [30], and a Bayesian-based approximation filter proposed in [31].

Most of the work done on bad data or cyber intrusion detection in power system is focused on state estimation application. However, to the best of our knowledge, PMU-enabled state estimators are yet to be integrated with the WAMS-based oscillation monitoring application. Therefore, detection techniques focused on state estimation cannot be applied here.

Kaveri Mahapatra and Nilanjan Ray Chaudhuri are with Department of Electrical Engineering, The Pennsylvania State University, State College, PA 16802, USA (e-mail: kzm221@psu.edu, nuc88@engr.psu.edu).

Financial support from NSF under grant awards CNS 1544621 and CNS 1739206 are gratefully acknowledged.

Our goal is to detect malicious injection of anomalous PMU data and correct the data stream for oscillation monitoring application.

Not many papers exist that focused on cyber-attack detection for the oscillation monitoring application in power systems. Reference [31] applied a Bayesian-based Approximated Filter (BAF) to extract modal damping and frequencies from corrupted data. In contrast to [31] and prior works focused on cyber intrusion detection in PMU data, this paper proposes an interface layer that pre-processes a window of data samples to detect data corruption stemming from cyber-attack or otherwise and reconstructs the data stream for wide-area monitoring applications. To that end, we propose to apply Principal Component Pursuit (PCP) method [32]–[34], which is solved using an augmented Lagrangian multiplier (ALM)-based algorithm [35], [36].

In reference [37], Principal Component Analysis (PCA) has been used to distinguish between fault outliers and bad data outliers, which have similar appearance as the former. However, the focus has only been on outlier detection.

In contrast to [37], the present work demonstrates the effectiveness of the proposed approach when different types of carefully designed cyber-attacks [31] corrupt PMU data. These include (1) data repetition attack, (2) missing data attack, (3) noise injection attack, (4) parameter manipulation attack, and (5) fault-resembling injection attack. The attacks on PMU data under ambient and transient condition has been considered. We have taken into account attack on a single stream of PMU data and multiple streams at a time, and demonstrated the reconstruction of the original PMU data from the corrupted data using PCP. The proposed approach allows the reconstructed data set to be post-processed by wide-area monitoring algorithms like Mode Meters.

Different mode metering algorithms like block-processing algorithms [38]–[40] and recursive algorithms [11], [41] can be applied to the reconstructed data stream. In this paper, a simple Recursive Least Squares (RLS) [42] algorithm has been applied as an example of mode metering technique to estimate the modal damping ratio and frequency. Effect of data corruption on modal estimation and the effectiveness of the proposed data reconstruction on improving the estimation accuracy is demonstrated using synthetic PMU data measured from a 16-machine 68-bus New-England New-York system.

II. PROPOSED ARCHITECTURE

We propose an architecture for malicious corruption-resilient wide-area monitoring, which is shown in Fig. 1. As shown in this figure, the proposed architecture relies on a data pre-processor based on the Principal Component Pursuit (PCP) approach. Phasor Data Concentrators (PDCs) situated at the control center align the data packets received from PMUs located at remote buses and pass on the data streams to the data pre-processor. We assume malicious injections through cyber-attacks can take place before the data arrives at the control center by overcoming communication layer security and that the control center is secure from such attacks.

Since the power system mostly operates under quasi-static condition, attack on the PMU data under this condition, also

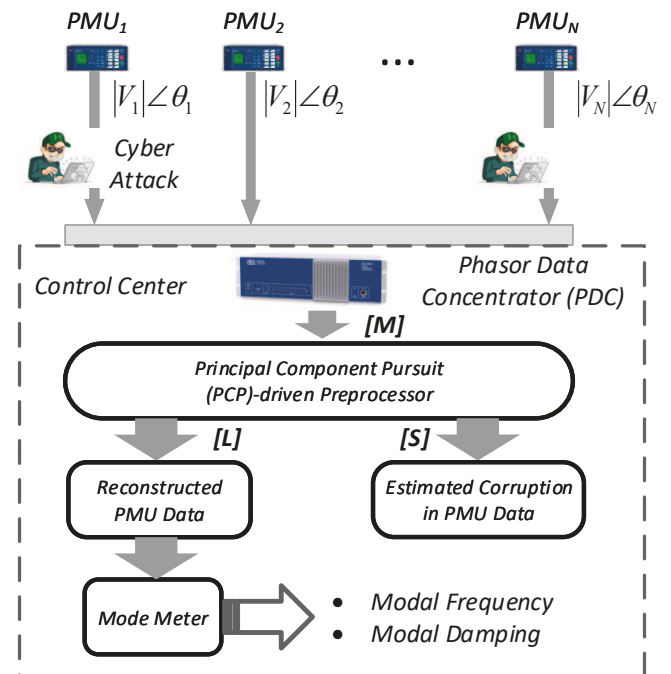


Fig. 1. Proposed architecture for malicious corruption-resilient wide-area oscillation monitoring algorithm.

known as ‘ambient data,’ will be taken into consideration. We consider the following types of attack under this condition -

1. *Parameter manipulation attack* - In this mode, attackers inject signals with altered modal characteristics, e.g. increased or decreased damping ratio.
2. *Fault-resembling injection attack* - In this mode, we assume that attackers got access to fault recordings from archived PMU data and injects the same in the ambient data.
3. *Noise injection attack* - In this mode, the attackers inject random Gaussian noise in the ambient data.

We have also considered cyber-attack in the transient PMU data following large disturbances. Three types of cyber-attacks were simulated for this condition -

1. *Data repetition attack* - In this case, the attackers extract a block of data from the ambient condition and repeats that in the transient condition.
2. *Missing data attack* - The attackers stop data samples from reaching the control center. Under this condition, PDC produces the latest available data sample repeatedly unless fresh samples appear.
3. *Noise injection attack* - The attack is similar to that mentioned for ambient data.

As shown in Fig. 1, the corrupted data is passed through the PCP-driven pre-processor, which is described next.

A. Principal Component Pursuit (PCP)-driven Preprocessor

Principal Component Analysis (PCA) [43], [44] is one of the most effective techniques used for dimensionality reduction, which approximates a given set of data points into a low-dimensional linear subspace. Principal components of the data are the set of orthogonal basis vectors of this subspace. A data matrix observed as a response from a linear system

over time can be presented as a combination of a low-rank matrix representing the underlying/actual subspace and a sparse matrix representing the corruption in the data, which is mostly noise in the measurements, any outliers, or spurious samples affecting a fraction of signals at any instance.

■ *Remark on Cyber Attack:* These spurious samples can originate from cyber attacks or intrusion during the normal system operation. It is assumed that the attackers can get access to a fraction of PMU data streams. We believe it will be highly difficult to get access to all PMU data streams. ■

The low rank matrix mentioned above consists of the basis vectors obtained from the system response and the sparse matrix represents the spurious perturbation in each position of the data matrix. In absence of corruption in the data, the best estimate of the low rank matrix in l_2 sense can be achieved by PCA via singular value decomposition and thresholding [32]. Moreover, in presence of an independently and identically distributed perturbations in the data matrix, PCA is able to obtain an optimal estimate of the underlying subspace that is stable with error bounded to be proportional to the magnitude of the perturbation. However, this is very sensitive to grossly corrupted observations [33].

On the contrary, Principal Component Pursuit (PCP) method guarantees to recover a low rank matrix from the data matrix despite gross sparse errors by solving a convex program [32]. The data matrix M can be represented as a sum of low rank matrix, L_0 and sparse matrix S_0 with very few nonzero entries at random locations. Unlike PCA, both L_0 and S_0 are allowed to have arbitrary magnitude without any rank specification for L_0 or support signs of S_0 . The following convex optimization problem which represents a weighted sum of the nuclear norm of the low-rank matrix L_0 and of the l_1 norm of the sparse matrix S_0 is solved by PCP to recover L_0 and S_0 from the data matrix M :

$$\begin{aligned} \min_{L, S} & \|L\|_* + \lambda \|S\|_1 \\ \text{subject to } & M = L + S \end{aligned} \quad (1)$$

where, λ is a positive regularization parameter, which controls the smoothness and sparseness of L and S , respectively. Here, $\|\cdot\|_*$ and $\|\cdot\|_1$ denote the nuclear norm, which is the sum of singular values; and the l_1 norm, which is the sum of absolute values of the elements of the matrix, respectively.

In order to make the approach more effective, the notions of the low rank matrix L being exactly low rank with no sparsity and sparse component matrix S being exactly sparse with the sparsity patterns being uniformly random are imposed in the problem [33]. Singular value decomposition of the low rank matrix $L_0 \in \mathbb{R}^{n_1 \times n_2}$ is given by:

$$L_0 = U \Sigma V^* = \sum_{i=1}^r \sigma_i u_i v_i^* \quad (2)$$

where ' r ' represents the rank of the matrix L_0 . $\sigma_1, \dots, \sigma_r$ denote the ' r ' singular values. The left and right singular vectors are given by $U = [u_1, \dots, u_r]$ and $V = [v_1, \dots, v_r]$, respectively.

A simple PCP solution can recover the low rank and sparse components provided the rank of the low rank matrix is not too large and the sparse component is reasonably sparse. The support of S_0 is defined as the set of indices of the nonzero

entries of the matrix. Here, $\|S_0\| = m$ represents the number of nonzero elements in the matrix. The identifiability issue of S_0 when it is a low rank matrix is avoided by the assumption of S_0 being uniformly random in being sparse among all the possible support of size ' m '. In this context, the PCP theorem presented in [33] is described below.

PCP Theorem [33]: "Suppose L_0 is $n \times n$, obeys incoherence property and that the support set of S_0 is uniformly distributed among all sets of cardinalities m . Then there is a numerical constant c such that with probability at least $1 - cn^{-10}$ (over the choice of support of S_0), Principal Component Pursuit with $\lambda = 1/\sqrt{n}$ is exact, i.e. $\hat{L} = L_0$ and $\hat{S} = S_0$, provided that

$$\text{rank}(L_0) \leq \rho_r n \mu^{-1} (\log n)^{-2} \quad (3)$$

$$m \leq \rho_s n^2 \quad (4)$$

Above, ρ_r and ρ_s are positive numerical constants. In the general rectangular case where L_0 is $n_1 \times n_2$, PCP with $\lambda = 1/\sqrt{n_{(1)}}$ succeeds with probability at least $1 - cn_{(1)}^{-10}$, provided that

$$\text{rank}(L_0) \leq \rho_r n_{(2)} \mu^{-1} (\log n_{(1)})^{-2} \quad (5)$$

$$m \leq \rho_s n_{(1)} n_{(2)} \quad (6)$$

where $n_{(1)} = \max(n_1, n_2)$ and $n_{(2)} = \min(n_1, n_2)$ ".

■ *Remark on Necessary & Sufficient Conditions:* The theorem implies, given the following three conditions

- a low rank matrix L_0 satisfies the incoherence property,
- a support set of S_0 is uniformly distributed among all sets of cardinality m , and
- the rank of L_0 satisfies the rank constraint and corruption is present only in a fraction of total number of elements in the matrix (see, equations (3)-(6));

the exact L_0 matrix can be recovered from their mixture with higher probability of success (nearly 1).

However, as shown in [45] the exact recovery of the data matrix with high probability of success is possible even if these conditions are violated. This implies that all these conditions are sufficient conditions, but by no means necessary conditions. Structure of corruption in the data is always unknown in advance and it is assumed that corruption has occurred in a fraction of the samples in the data matrix. ■

■ *Remark on Incoherence Property:* The procedure to calculate the coherence of a matrix and whether the data matrix L_0 satisfies the incoherence property is mentioned below [34].

Let U be a subspace of \mathbb{R}^n of dimension ' r ' and P_U be the orthogonal projection onto U . Then the coherence of U is defined as

$$\mu(U) = \frac{n}{r} \max_{1 \leq i \leq n} \|P_U e_i\|^2 \quad (7)$$

$$\text{where } P_U = \sum_{i \in [r]} u_i u_i^* = U U^*$$

$\mu(V)$ can be calculated in a similar way and the coherence parameters for L_0 can be found as

$$\mu_0 = \max(\mu(U), \mu(V)) \quad (8)$$

$$\mu_1 = \mu_0 \sqrt{r} \quad (9)$$

For any subspace, the largest possible value for μ is n/r and the smallest value that can be achieved is 1. Incoherence condition asserts that for smaller values of μ , the singular values are reasonably spread out. The incoherence condition states,

$$\max_i \|U^* e_i\|^2 \leq \frac{\mu_0 r}{n_1}, \max_i \|V^* e_i\|^2 \leq \frac{\mu_0 r}{n_2}, \quad (10)$$

where, U and V are obtained from SVD of L_0 , and the canonical basis vectors are given by e_i 's. The LHS terms must satisfy the above two conditions with some positive smaller values of coherence parameter μ . The third condition is

$$\|UV^*\|_\infty \leq \mu_1 \sqrt{\frac{r}{n_1 n_2}} \quad (11)$$

This incoherence condition implies that the maximum entry of absolute values of the elements of the matrix UV^* must be bounded by the term in the RHS. ■

■ *Remark on Corruption & Rank Properties:* References [33] and [45] have conducted experiments without assuming any specific structure on the support set, which still gave appealing results. This implies that the truth of getting results with PCP is beyond what can be proved by assuming a specific structure to the error [33]. Also, in real life, there is no way to know in advance about the structure of corruption in S_0 and the uncorrupted L_0 , which is different based on the type of application. Candes et-al [33] do not guarantee that PCP will succeed with high probability of success all the time in reconstructing the low rank matrix, but references [33] and [45] provide enough evidence of recovering the low rank matrix with high probability and minimum error.

In this work, we have performed extensive experiments on the power system measurements through different corruption patterns, which lead to similar conclusions. The caveat however is that the PCP works if the corruption is not present in all the variables at the same time. From an engineering perspective, if the attacks corrupt most of the data, or are aimed at the common communication links or the control center, the method will not reconstruct the signals efficiently. The method works based on the fact that the original behavior of the corrupted signals can be recovered at any instant by accounting current behavior of the uncorrupted signals and past behavior of all signals, via capturing the low rank subspace for the present data window. If all the samples considered at any instant are corrupted, there is no way to predict the signal trajectories. This in turn demands solving a time series prediction problem based on the past behavior of the signals over a long period of time. Therefore, a complete corruption will translate the problem into time-series prediction problem from data anomaly detection, which is outside the scope of this paper. The attack model in this work assumes that an attacker does not have access to all the nodes at the same time. ■

Various efficient and scalable algorithms with computational burden no more than classical PCA have been proposed for solving PCP. These include accelerated proximal gradient approach [46] and iterative thresholding approach [47]. In this work, an augmented Lagrangian multiplier (ALM)-based algorithm [35], [36] has been utilized to solve the problem in equation (1). The advantages of ALM include higher accuracy in fewer iterations and applications in wide range of problem settings without many tuning parameters. Further, the bound on the rank of the iterates remains within the rank of L_0 during the optimization, which results in efficient computation of the solution.

The constrained optimization problem is solved by converting it to an unconstrained optimization problem with a new objective called the augmented Lagrangian which is given by:

$$l(L, S, Y) = \|L\|_* + \lambda \|S\|_1 + \langle Y, M - L - S \rangle + \frac{\mu}{2} \|M - L - S\|_F^2 \quad (12)$$

where, the Lagrange multiplier matrix is given by Y and μ denotes the single regularization parameter associated with the ALM formulation.

The ALM-based objective formulation for PCP problem is given by [33]:

$$\begin{aligned} \text{minimize } l(L, S, Y) = & \|L\|_* + \lambda \|S\|_1 + \langle Y, M - L - S \rangle \\ & + \frac{\mu}{2} \|M - L - S\|_F^2 \end{aligned} \quad (13)$$

A generic Lagrange multiplier algorithm-based method [48] can be used to solve the above problem in several iterations in which each iteration consists of two steps. The subproblem in equation (14) is solved in the first step to get L_k and S_k :

$$(L_k, S_k) = \text{argmin}_{L, S} l(L, S, Y_k) \quad (14)$$

The Lagrange multiplier matrix Y_k is updated with the residual $M - L - S$ in the second step:

$$Y_{k+1} = Y_k + \mu(M - L_k - S_k) \quad (15)$$

Due to the unavailability of the optimal solution for the subproblem in the first step, a practical and efficient optimization method based on alternating directions is employed to find the solutions in the first step with several interstep iterations. The following two substeps are repeated alternatively to attain convergence to the optimal solution. In one substep, $l(L, S, Y_k)$ is minimized with respect to L with S fixed and in another substep $l(L, S, Y_k)$ is minimized with respect to S with L fixed. This assumes attaining closed form solutions for the fixed value in each substep iterations. However, for reducing the computational burden this can be solved once instead of repeating which is sufficient to converge to optimal solution [35]. This is achieved by solving the following:

$$\arg \min_S l(L, S, Y) = S_{\lambda \mu^{-1}} (M - L + \mu^{-1} Y) \quad (16)$$

and

$$\arg \min_L l(L, S, Y) = D_{\mu^{-1}} (M - S + \mu^{-1} Y) \quad (17)$$

where, $S_\tau : \mathbb{R} \rightarrow \mathbb{R}$ is a shrinkage operator represented by:

$$S_\tau [x] = \text{sgn}(x) \max(|x| - \tau, 0) \quad (18)$$

with the threshold value given by $\tau > 0$. When extended to matrices, this operator is applied to each element in the matrix and is given by:

$$S^* = \arg \min_S l(L, S, Y) = S_{\lambda, \mu^{-1}}(D - L + \mu^{-1}Y) \quad (19)$$

and $D_\tau(X)$ is the singular value thresholding operator and is given by

$$D_\tau(x) = U S_\tau(\Sigma) V^* \quad (20)$$

where, $X = U \Sigma V^*$ represents the singular value decomposition of X .

$$L^* = \arg \min_L l(L, S, Y) = D_{\mu^{-1}}(D - S + \mu^{-1}Y) \quad (21)$$

The steps of the complete algorithm [33] are as follows:

- 1) initialize: $S_0 = Y_0 = 0, \mu > 0$
- 2) while not converged, do
 - (a) Compute $L_{k+1} = D_{\mu^{-1}}(M - S_k + \mu^{-1}Y_k)$;
 - (b) Compute $S_{k+1} = S_{\lambda, \mu^{-1}}(M - L_{k+1} + \mu^{-1}Y_k)$;
 - (c) Compute $Y_{k+1} = Y_k + \mu(M - L_{k+1} - S_{k+1})$;

3) end while

4) output: L, S

In this work, the above algorithm is utilized to solve PCP.

■ **Remark on $[M]$, $[L]$, and $[S]$:** As shown in Fig. 1, the input to PCP is matrix $[M]$ (see, eqn. (1)), which consists of time-series voltage phasor data obtained from PMUs. The phasor data includes n_2 time-samples of voltage magnitudes and corresponding phase angles from $n_1/2$ buses where PMUs are placed constituting an $n_1 \times n_2$ matrix. For example, the test system described in Section IIIA, 10 PMUs are considered with 20s window during transient case and 50s window during ambient case. These lead to a 20x1200 and a 20x2994 element matrices, respectively, with the assumption of PMU output at 60Hz sampling.

Note that the output of the above algorithm are the matrices representing reconstructed signals $[L]$ and the estimated corruption in PMU data $[S]$ - please see Fig. 1. Following the reconstruction of the PMU signals it is analyzed by mode metering algorithms to estimate modal frequency and damping ratio. ■

B. Modal Estimation

As described in the Introduction, different algorithms can be used for modal estimation. In this work, we have applied the well-known Recursive Least Squares (RLS) algorithm [42]. We use a variable forgetting factor-based algorithm [42], which is well-known and is not repeated here.

C. Engineering Insights

The paper considers wide-area monitoring of low frequency oscillations as the application area, which needs to estimate the modal frequency and damping ratio in near real-time. This gives the operators situational awareness and acts as an early warning system for proactive re-dispatch-based control, which is named as Modal Analysis for Grid Operations

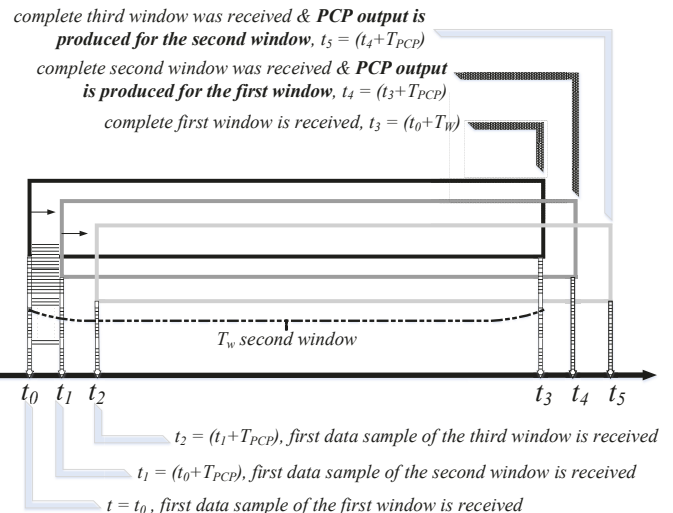


Fig. 2. Proposed ‘Overlapping Window’ framework.

(MANGO) [9], [10]. The MANGO scheme has been successfully implemented in BPA’s control room [9], [10].

The PCP algorithm is ‘Block-Processing’ in nature and will work in an ‘Overlapping Window’ framework shown in Fig. 2. The window size (T_W seconds) can be determined as a tradeoff between the accuracy of PCP vs the computational burden it poses. Let us consider a case where the control center has only one dedicated processor for executing the PCP algorithm, which takes T_{PCP} seconds to produce output $[L]$ and $[S]$. While the PCP algorithm is executed, the next window will overlap with $(T_W - T_{PCP})$ seconds of data from the previous window and take into account T_{PCP} seconds of new data samples. This will ensure that there is always a time lag of T_{PCP} seconds before the data is used by modal estimation algorithms. In Section III, we will demonstrate the T_W -vs-accuracy tradeoff and calculate the corresponding T_{PCP} values. We will show that a $T_W = 50$ s window produces acceptable accuracy in reconstruction while the corresponding time lag incurred (T_{PCP}) will be less than 2.0s.

Therefore, when a new data sample arrives, e.g. right after the first window in Fig. 2, it will take T_{PCP} seconds following that instant to fill the second window. In addition, a further T_{PCP} seconds will lapse for PCP computation before the data is ready for processing by modal estimation algorithms. This implies that the maximum possible delay between the instance of the incoming data sample and PCP output is $2T_{PCP}$. However, with respect to the last sample in the second window, the delay is T_{PCP} . **Therefore, the average delay between the instant of the incoming data samples and PCP output is $1.5T_{PCP}$, which is less than 3.0s.** This should be reasonable for near real-time applications.

Notably, this is assuming we have only a single dedicated processor working with one window of data at a time and completing the task in T_{PCP} seconds before processing the next window. With parallel processing capability, this delay can be further reduced. Also, lesser T_W leads to slightly poorer accuracy, but shorter delay. Figure. 2 shows this process.

If a Block-Processing modal estimation algorithm [38]–[40] is used, it will work on the latest reconstructed data matrix $[L]$.

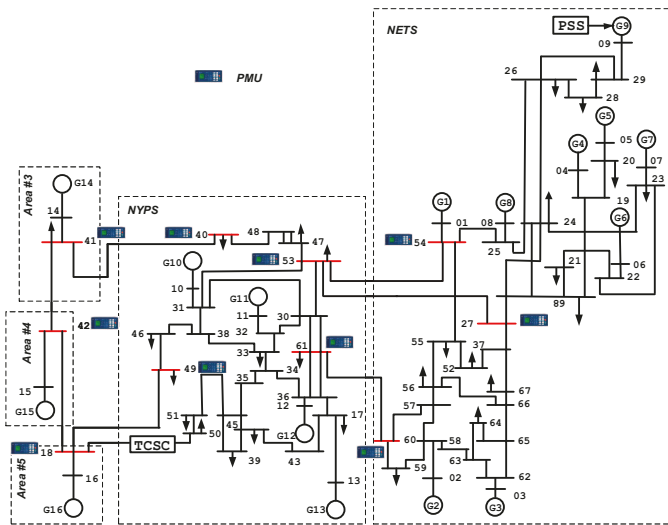


Fig. 3. Single-line diagram of 16-machine, 5-area New England-New York system with PMUs installed at major inter-tie buses highlighted in red.

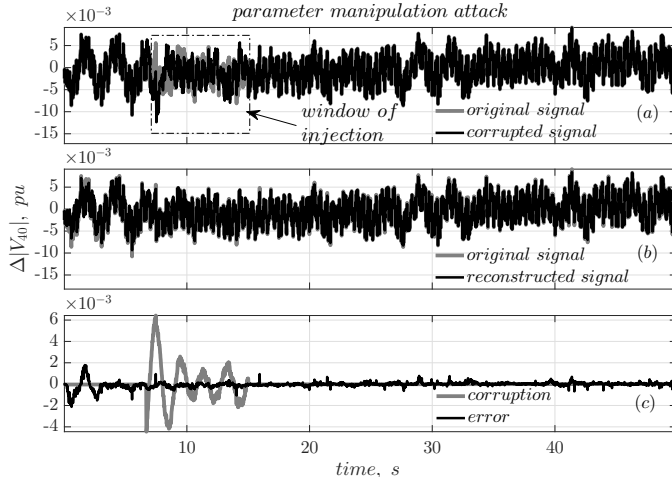


Fig. 4. Case IA: Parameter manipulation attack in signal $|V_{40}|$ under ambient condition. Corruption: difference between original and corrupted signal, Error: difference between original and reconstructed signal.

On the contrary, a Recursive modal estimation technique like RLS in this paper, will work on the new data samples of the $[L]$ matrix corresponding to the latest T_{PCP} seconds.

III. CASE STUDY

A. Test System

We have considered a positive-sequence fundamental frequency phasor model of the 16-machine, 5-area New England-New York system [49] with PMUs installed at major inter-tie buses highlighted in red, which are shown in Fig. 3. A PMU data rate of 60Hz is assumed. Ten voltage magnitudes and corresponding voltage angles (i.e. twenty signals) were considered in this study and de-trending was performed on all signals before solving PCP. The objective of the Mode Meter is to estimate two critical inter-area modes with frequencies 0.382Hz and 0.618Hz, and corresponding damping ratios 6.5% and 5.7%, respectively. In Appendix A, we have shown that the uncorrupted power system measurement matrix L_0 satisfies the incoherence property described in equations (10) and (11).

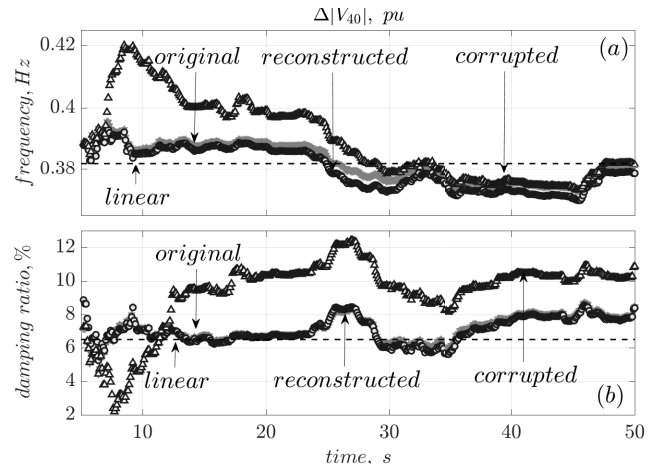


Fig. 5. Case IA: Estimated frequency and damping ratio from corrupted (Δ) signal is misleading. Reconstruction (\circ) produces reasonable accuracy as compared to original (grey $*$).

We have considered cyber-attacks on PMU data under (1) ambient condition, and (2) transient condition, which are described below.

1) *Ambient Condition*: To simulate the ambient condition, band-limited zero-mean gaussian noise was injected in load terminals of the power system. Next, the effectiveness of the proposed approach is demonstrated with different cases of cyber-attacks.

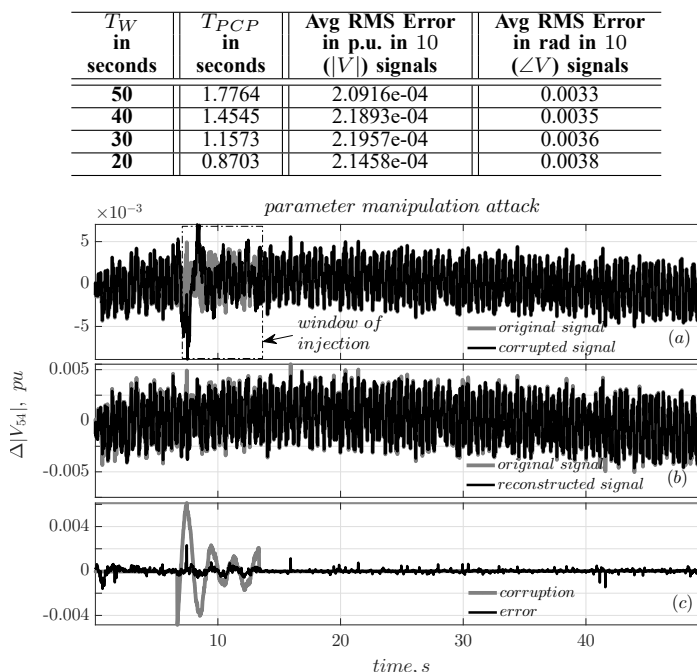
■ Case IA: Parameter Manipulation Attack on One Signal:

First, we consider attack on one variable. Figure 4 shows the parameter manipulation attack in signal $|V_{40}|$. Unless otherwise stated, only deviation in the signals from nominal condition are shown. The attack model uses the weighted sum of three damped sinusoids with frequencies equal to 0.382Hz, 0.55Hz, and 0.618Hz. The damping ratios are chosen to be 8.0%, 4.4%, and 5.7%, respectively. Figure 4(c) compares the degree of malicious injection in the signal and the quality of reconstruction. These are measured by the difference between the original and the corrupted signal denoted by 'corruption,' and the difference between original and reconstructed signal denoted by 'error.' The error is close to zero, which shows good quality of reconstruction.

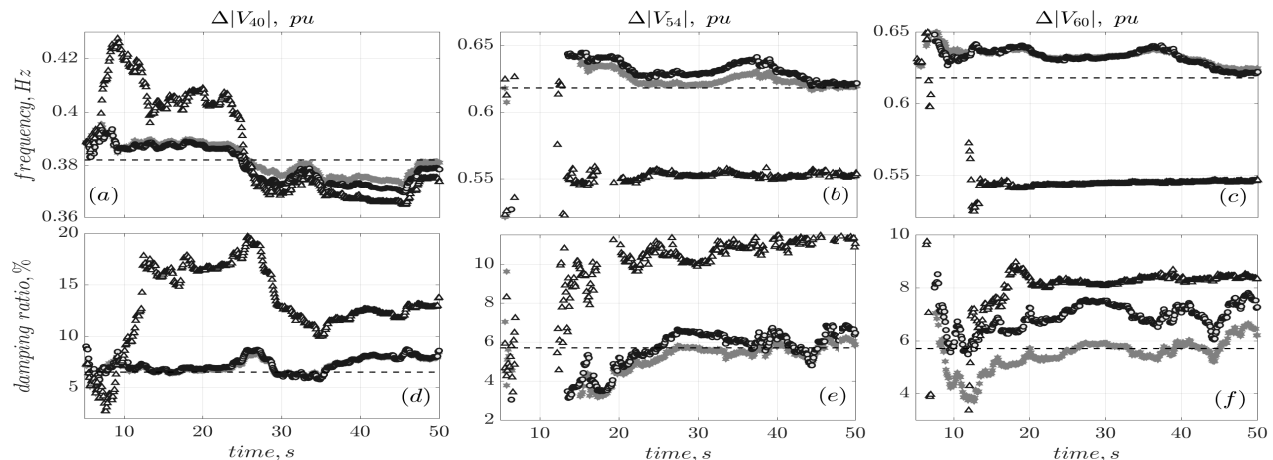
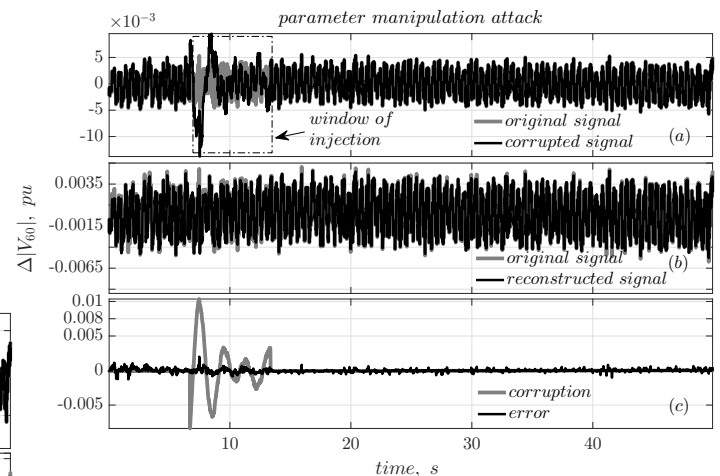
Figure 5 shows that the modal damping and frequency estimated by RLS algorithm from original signal (grey $*$) and the reconstructed signal (\circ) closely follow the values obtained from linear analysis. It also shows that a small window of corrupted data (Fig. 4(a)) can jeopardize the estimates (Δ) and give out misleading information. It is well-known that the RLS algorithm is sensitive to corruption in the signal and it has a prolonged effect, especially on the damping estimates – see for example [41]. The error in estimates prolong well beyond the disappearance of the corruption, since the RLS algorithm is '**Recursive**' in nature, i.e. its estimated parameter vector in the k^{th} sample is updated based on the $(k-1)^{th}$ sample.

Table I shows CPU time (T_{PCP}) vs accuracy trade-off of PCP algorithm with different window sizes (T_W) for Case IA. The proposed measure of accuracy is defined as the average of the RMS values of the error in each reconstructed

TABLE I

CASE IA: CPU TIME (T_{PCP}) VS ACCURACY TRADE-OFF OF PCP ALGORITHM WITH DIFFERENT WINDOW SIZE (T_W)Fig. 6. Case IB: Parameter manipulation attack in signal $|V_{54}|$ under ambient condition. Corruption: difference between original and corrupted signal, Error: difference between original and reconstructed signal.

signal. For example, the estimation error in signal $\Delta|V_{40}|$ is shown in Fig. 4(c). The average values of the RMS error for the reconstructed voltage magnitudes, $|V|$, and phase angles, $\angle V$ are presented separately in Table I. All the codes are executed in MATLAB R2016 environment using Intel Core *i7* processor with 16 GB RAM. The CPU time, T_{PCP} and error are calculated for window sizes of 50s, 30s, 40s, and 10s. As shown in Table I, T_{PCP} decreases with a decrease in window size, T_W . However, the average RMS error increases with decreasing window size. Therefore, a reasonable decision would be to keep the window size higher, such as 50 seconds for ambient cases. Note that, a $T_W = 50$ s window produces acceptable accuracy in reconstruction while the corresponding time lag incurred (T_{PCP}) is less than 2.0s, which should be

Fig. 8. Case IB: Estimated frequency and damping ratio from corrupted (Δ) signal is misleading. Reconstruction (\circ) produces reasonable accuracy as compared to original ($*$).Fig. 7. Case IB: Parameter manipulation attack in signal $|V_{60}|$ under ambient condition. Corruption: difference between original and corrupted signal, Error: difference between original and reconstructed signal.

reasonable for near real-time applications.

TABLE II
CASE IB: CPU TIME (T_{PCP}) VS ACCURACY TRADE-OFF OF PCP ALGORITHM WITH DIFFERENT WINDOW SIZE (T_W)

T_W in seconds	T_{PCP} in seconds	Avg RMS Error in p.u. in 10 ($ V $) signals	Avg RMS Error in rad in 10 ($\angle V$) signals
50	1.7768	2.1365e-04	0.0033
40	1.4466	2.2510e-04	0.0034
30	1.1739	2.3648e-04	0.0035
20	0.8788	2.8860e-04	0.0037

■ **Case IB: Parameter Manipulation Attack on Multiple Signals:** We consider parameter manipulation attack simultaneously on 3 signals - $|V_{40}|$, $|V_{54}|$, and $|V_{60}|$. Figures 6 and 7 show two of those signals, which highlight acceptable accuracy of the reconstructed signals as viewed from Figs 6(c) and 7(c).

Figure 8 shows that estimated damping and frequency from the reconstructed signals are quite accurate. Modal frequency and damping ratios estimated from each corrupted signal deviates from the actual values and if used, the hackers could be successful in convincing operators that the system damping has improved (Figs 8(d), (e), (f)).

Table II shows the CPU time (T_{PCP}) vs accuracy trade-off of PCP algorithm with different window sizes (T_W) for

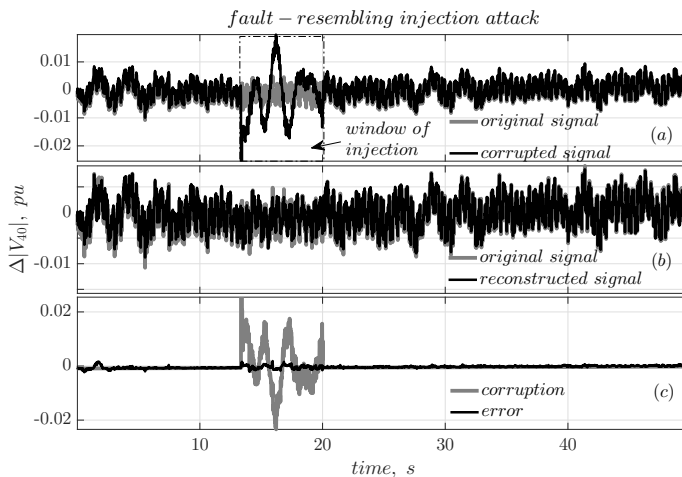


Fig. 9. Case II: Fault-resembling injection attack in signal $|V_{40}|$ under ambient condition. Corruption: difference between original and corrupted signal, Error: difference between original and reconstructed signal.

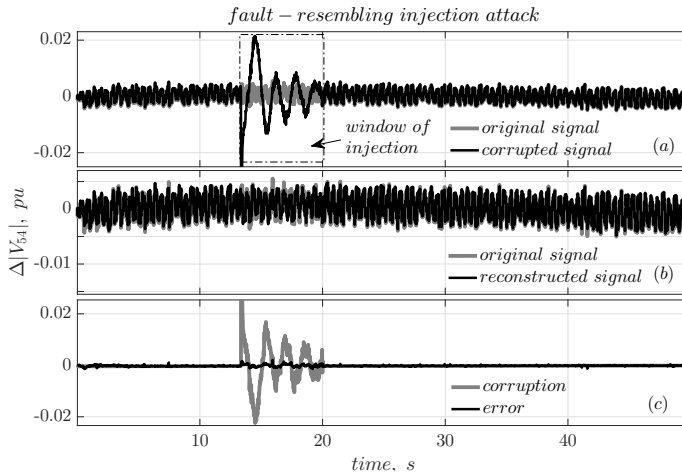


Fig. 10. Case II: Fault-resembling injection attack in signal $|V_{54}|$ under ambient condition. Corruption: difference between original and corrupted signal, Error: difference between original and reconstructed signal.

the case of parameter manipulation attack on multiple signals during ambient condition. The trend observed is consistent with the previous case.

■ **Case II: Fault-Resembling Injection Attack on Multiple Signals:** In this case, the attacker is assumed to inject a portion of archived transient data following a three-phase self-clearing

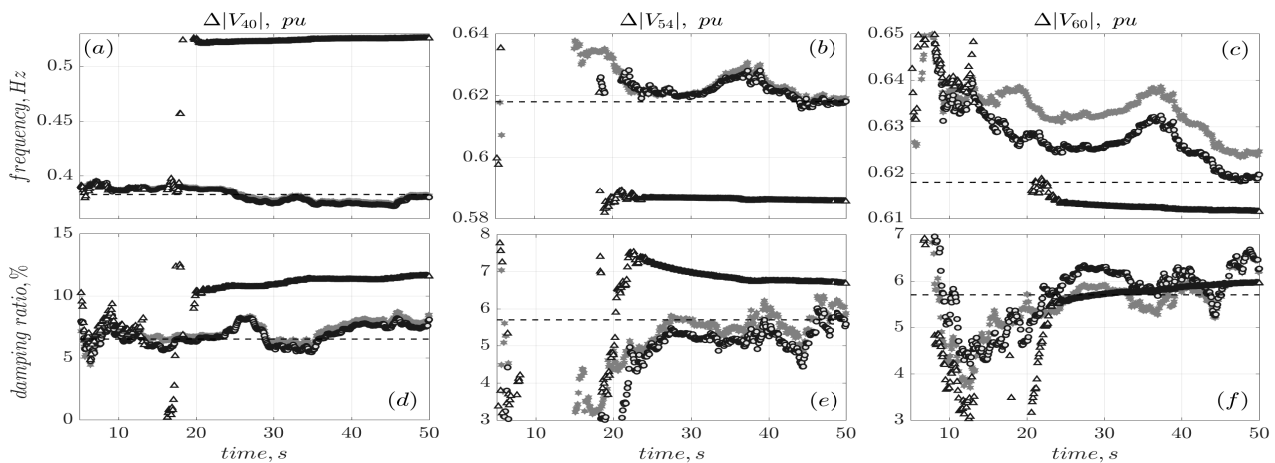


Fig. 11. Case II: Estimated frequency and damping ratio from corrupted (Δ) signal is misleading. Reconstruction (\circ) produces reasonable accuracy as compared to original ($*$).

TABLE III
CASE II: CPU TIME (T_{PCP}) VS ACCURACY TRADE-OFF OF PCP ALGORITHM WITH DIFFERENT WINDOW SIZE (T_W)

T_W in seconds	T_{PCP} in seconds	Avg RMS Error in p.u. in 10 ($ V $) signals	Avg RMS Error in rad in 10 ($\angle V$) signals
50	1.7836	2.7513e-04	0.0033
40	1.4405	2.9730e-04	0.0034
30	1.1686	3.1385e-04	0.0035
20	0.8758	3.7680e-04	0.0037

TABLE IV
CASE III: CPU TIME (T_{PCP}) VS ACCURACY TRADE-OFF OF PCP ALGORITHM WITH DIFFERENT WINDOW SIZE (T_W)

T_W in seconds	T_{PCP} in seconds	Avg RMS Error in p.u. in 10 ($ V $) signals	Avg RMS Error in rad in 10 ($\angle V$) signals
50	1.7437	2.2931e-04	0.0033
40	1.4423	2.5575e-04	0.0035
30	1.1691	3.2689e-04	0.0036
20	0.9258	4.4798e-04	0.0038

fault near bus 53 into three signals $|V_{40}|$, $|V_{54}|$, and $|V_{60}|$. Due to space restriction, two of these injections are shown in Figs 9 and 10. The quality of reconstruction is very good and is reflected in the estimated frequency and damping ratios in Fig. 11. Since the injected signals are actual transient response from the system, estimates from the corrupted signals finally tend to converge to original values. However, due to transient signal injection, a large deviation is witnessed in all estimates obtained from corrupted signals.

Table III shows the CPU time and average RMS error in the recovered signals after execution of PCP algorithm for the case of fault-resembling injection attack on multiple signals during ambient condition. The trend observed in CPU time and error is consistent with the previous cases.

■ **Case III: Noise Injection Attack on Multiple Signals:** A noise injection attack is simulated by replacing data samples with zero mean Gaussian white noise on 3 signals - only one is shown in Fig. 12. Figure 13 shows that the damping and frequency estimation from the reconstructed data is quite accurate.

Table IV shows the CPU time and average RMS error in the recovered signals after execution of PCP algorithm for the case of noise injection attack on multiple signals during ambient

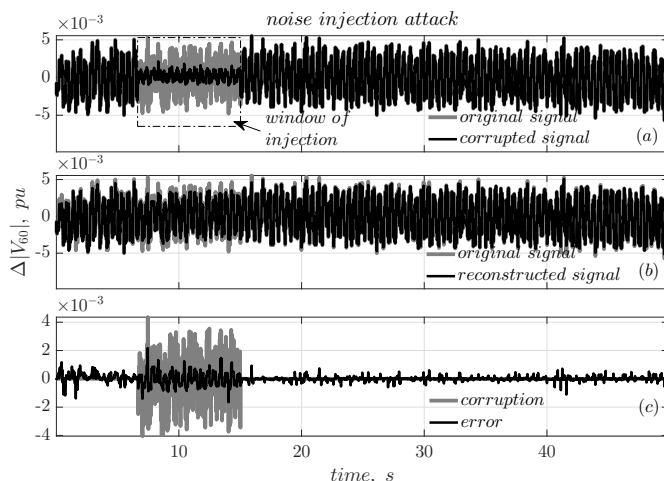


Fig. 12. Case III: Noise injection attack in signal $|V_{60}|$ under ambient condition. Corruption: difference between original and corrupted signal, Error: difference between original and reconstructed signal.

condition. Similar observations can be made as before.

2) *Transient Condition*: Figure 14 shows the system response following a self-clearing three-phase fault near bus 53 - only four signals out of twenty are shown here. We will disregard the first half-cycle of oscillatory data immediately after fault to avoid the effect of higher nonlinearity and initiate the window following that for application of PCP. This is acceptable since the accuracy of most of the mode-metering algorithms is poor in this region.

■ *Case IV: Noise Injection Attack on One Signal*: Similar to Case III, Gaussian noise injection attack following the transient event is considered on one signal. As shown in Fig. 15 the error in the reconstructed signal is higher at the beginning of the window. However, it is acceptable in most of the portion of the window. This can be attributed to a higher degree of nonlinearity in the temporal proximity of the fault event.

Figure 16 shows the estimated modal frequency and damping ratio from the original, corrupted, and reconstructed signals. The corruption in the signal leads to a frequency estimate, which is lower than the actual frequency. More importantly, the damping ratio estimation from the corrupted signal leads us to believe that the system is better damped. The estimates

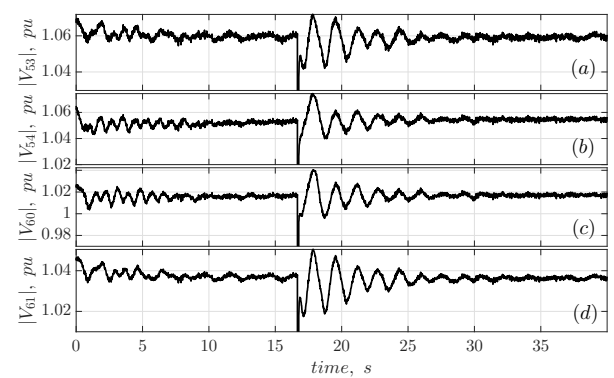


Fig. 14. Typical voltage magnitude signals following a self-clearing fault near bus 53.

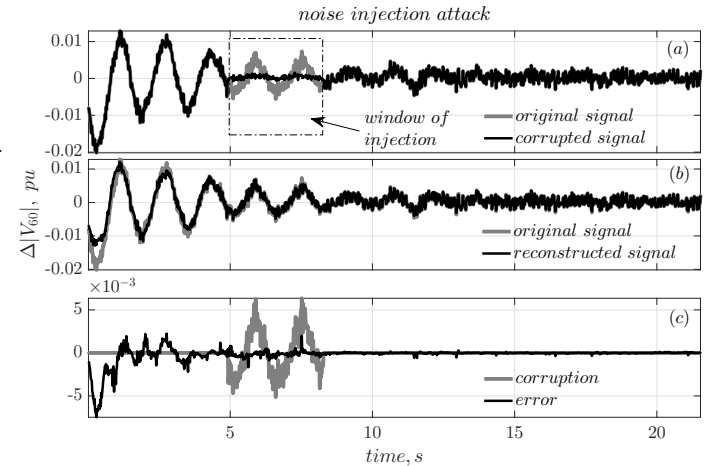


Fig. 15. Case IV: Noise injection attack attack in signal $|V_{60}|$ under transient condition. Corruption: difference between original and corrupted signal, Error: difference between original and reconstructed signal.

obtained from the reconstructed signal very closely resembles the estimates obtained from the original signal (15(b)).

■ *Case V: Missing Data Attack on Multiple Signals*: We consider a missing data attack on 3 PMU signals - $|V_{54}|$, $|V_{60}|$, $|V_{61}|$. The effectiveness of the proposed pre-processor in data reconstruction is shown for two of those signals in Figs 17 and 18. Figure 19 compares the estimated values of frequency and damping ratio obtained from the original, corrupted, and

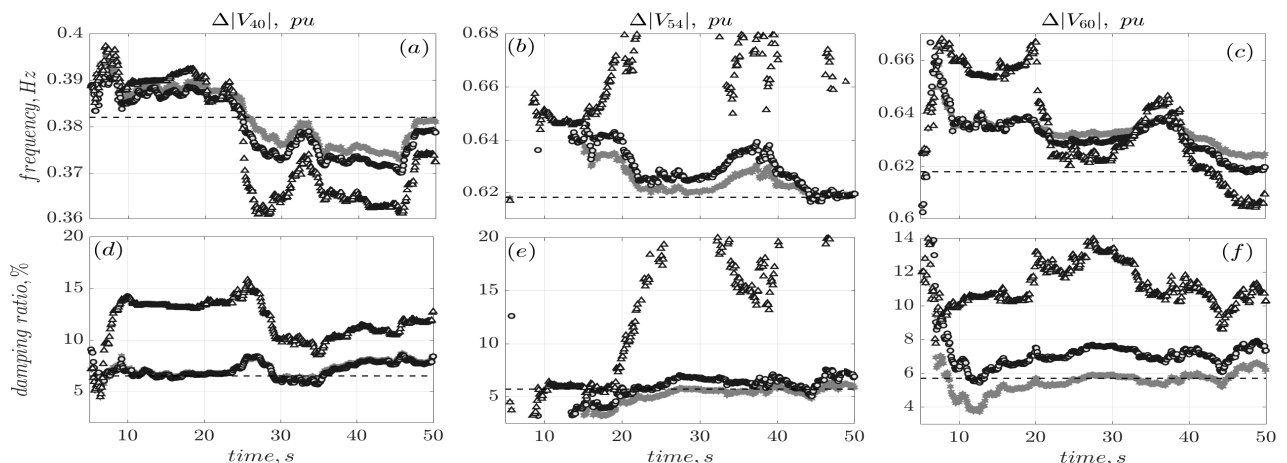


Fig. 13. Case III: Estimated frequency and damping ratio from corrupted (Δ) signal is misleading. Reconstruction (\circ) produces reasonable accuracy as compared to original ($*$).

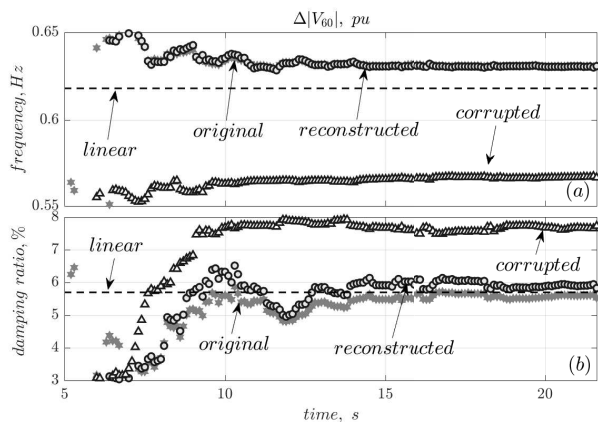


Fig. 16. Case IV: Estimated frequency and damping ratio from corrupted (Δ) signal is misleading. Reconstruction ('o') produces reasonable accuracy as compared to original (grey '*').

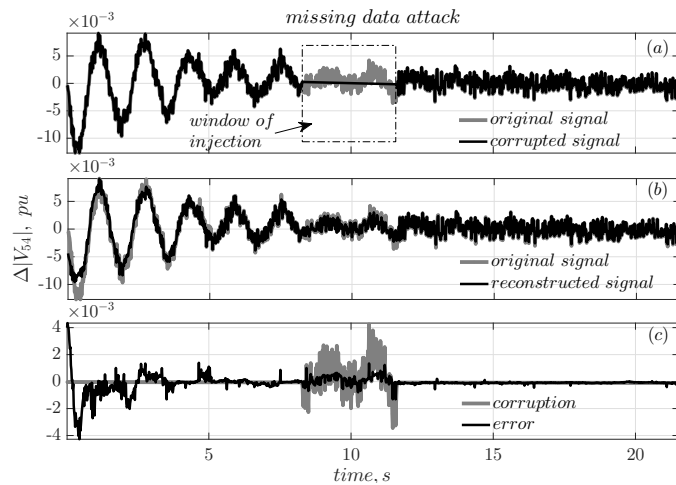


Fig. 17. Case V: Missing data attack in signal $|V_{54}|$ under transient condition. Corruption: difference between original and corrupted signal, Error: difference between original and reconstructed signal.

reconstructed signals. It can be seen that the corruption did not affect the estimates to a great extent. The estimates obtained from reconstructed data is pretty close to those obtained from the original signals.

■ **Case VI: Data Repetition Attack on Multiple Signals:** In this case a window of ambient data is repeated in the transient condition in 3 signals - $|V_{54}|$, $|V_{60}|$, and $|V_{61}|$. Figure 20 shows one of these signals. Like previous cases, the error in the reconstructed signal is higher at the beginning of the window,

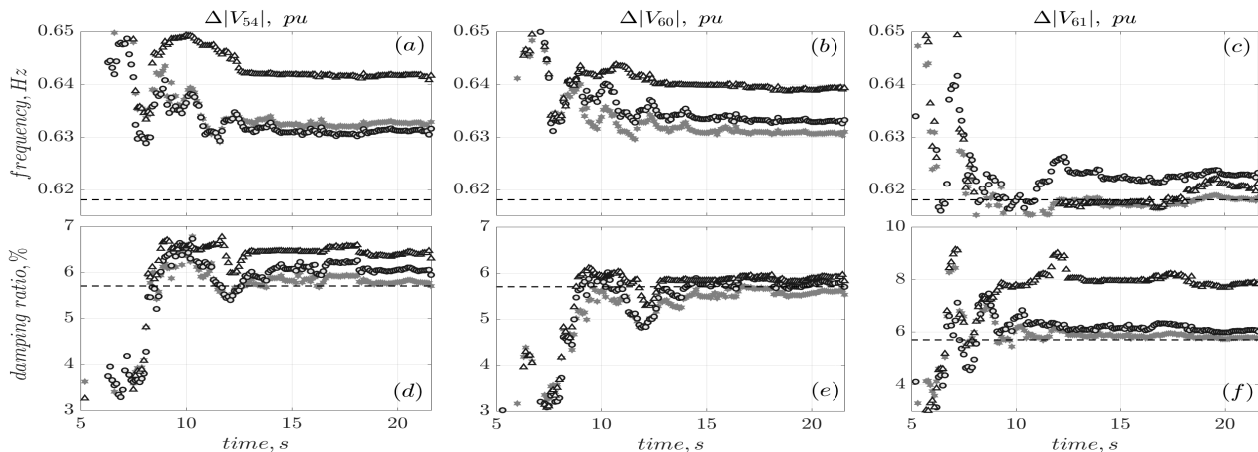


Fig. 19. Case V: Estimated frequency and damping ratio from original (grey '*'), corrupted (' Δ '), and reconstructed ('o') signals.

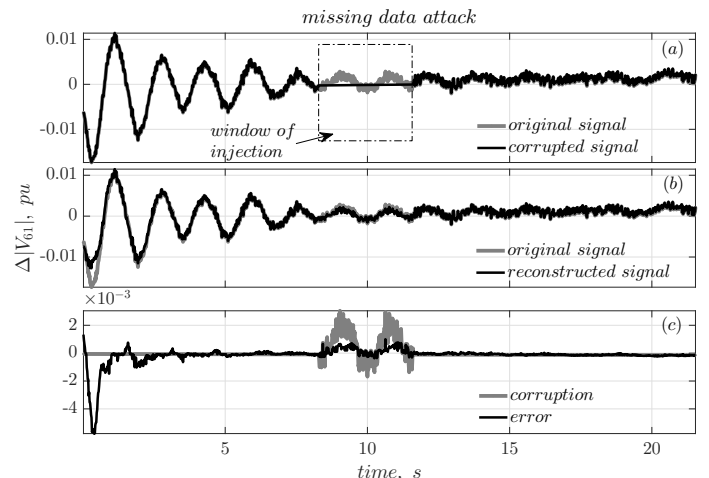


Fig. 18. Case V: Missing data attack in signal $|V_{61}|$ under transient condition. Corruption: difference between original and corrupted signal, Error: difference between original and reconstructed signal.

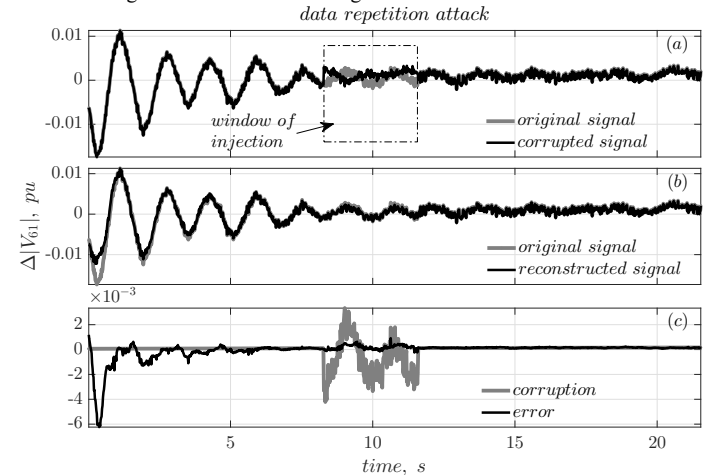


Fig. 20. Case VI: Data repetition attack attack in signal $|V_{61}|$ under transient condition. Corruption: difference between original and corrupted signal, Error: difference between original and reconstructed signal.

TABLE V
CASE IV: CPU TIME (T_{PCP}) AND ACCURACY OF PCP ALGORITHM WITH 20S WINDOW SIZE (T_W)

T_W in seconds	T_{PCP} in seconds	Avg RMS Error in p.u. in 10 ($ V $) signals	Avg RMS Error in rad in 10 ($\angle V$) signals
20	0.8760	5.7029e-04	0.0125

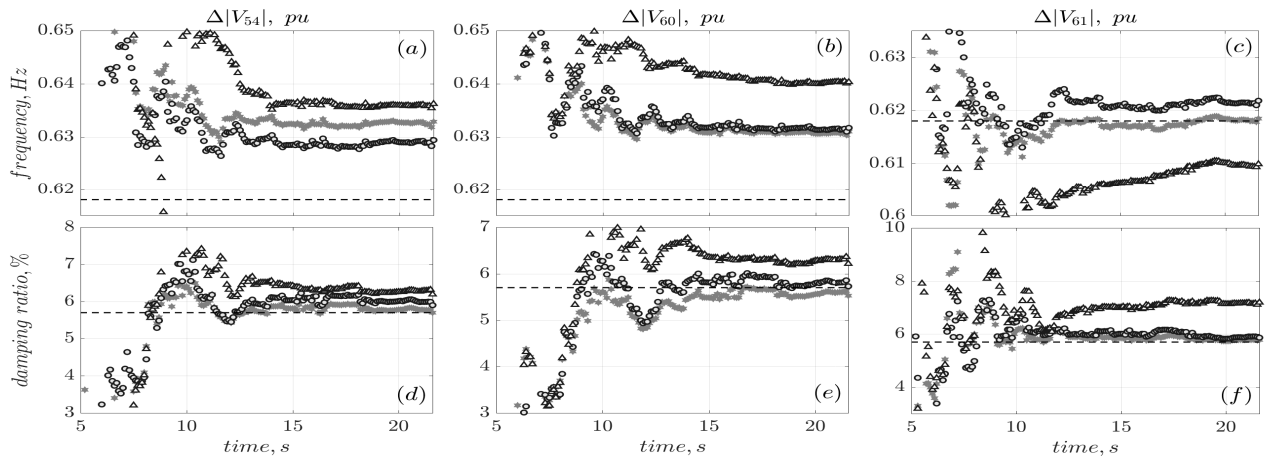


Fig. 21. Case VI: Estimated frequency and damping ratio from original (grey ‘*’), corrupted (‘Δ’), and reconstructed (‘o’) signals.

but is acceptable for most of the time span. It can be seen from Fig. 21 that the corruption in data consistently led to an increase in estimated damping ratio. The frequency and the damping estimates from the reconstructed signals appear to reasonably follow those obtained from the original signals.

Table V, Table VI, and Table VII show the CPU time and average RMS error in the recovered signals after execution of PCP algorithm for different cases of attacks during transient condition. A window size of 20 seconds is considered reasonable for recovering signals during transient condition.

TABLE VI

CASE V: CPU TIME (T_{PCP}) AND ACCURACY OF PCP ALGORITHM WITH 20S WINDOW SIZE (T_W)

T_W in seconds	T_{PCP} in seconds	Avg RMS Error in p.u. in 10 ($ V $) signals	Avg RMS Error in rad in 10 ($\angle V$) signals
20	0.8924	5.6413e-04	0.0125

TABLE VII

CASE VI: CPU TIME (T_{PCP}) AND ACCURACY OF PCP ALGORITHM WITH 20S WINDOW SIZE (T_W)

T_W in seconds	T_{PCP} in seconds	Avg RMS Error in p.u. in 10 ($ V $) signals	Avg RMS Error in rad in 10 ($\angle V$) signals
20	0.9152	5.6622e-04	0.0125

IV. CONCLUSION

Different types of malicious data corruption stemming from cyber-attack can jeopardize the estimation of damping ratios and frequencies of electromechanical modes. In this paper an approach for wide-area oscillation monitoring was presented, which is resilient to corruption in PMU data due to cyber-attack or otherwise. To that end, a Principal Component Pursuit (PCP)-driven interface was proposed between raw synchrophasor data and the algorithms used for wide-area monitoring application. It was shown that the PCP-based pre-processor can successfully detect the data corruption and reconstruct the original signal with acceptable accuracy, which in turn led to improved estimation of poorly-damped modes. A recursive oscillation monitoring algorithm was tested to validate the effectiveness of the proposed approach under both ambient and transient conditions.

APPENDIX

A. Incoherence property assumption of power system measurement matrix, L_0

We now show that the uncorrupted power system measurement matrix L_0 considered in the paper satisfies the incoherence property. The incoherence property has been tested for the data matrix used for applying PCP during transient and during ambient conditions.

Ambient: The data matrix of size $20(n_1) \times 2994(n_2)$ is considered, which resulted in the following μ values:

$$\mu_0 = \max \{ \mu(U) = 1, \mu(V) = 22.6129 \}$$

These are much smaller as compared to the maximum value of $n/r = 149.7$. Other values for testing the incoherence property are as follows:

$$\mu_0 = 22.6129, \quad \mu_1 = 101.1281, \quad \max_i \|U^* e_i\|^2 = 1, \\ \max_i \|V^* e_i\|^2 = 0.1511, \quad \|UV^*\|_\infty = 0.3261, \quad \mu_1 \sqrt{\frac{r}{n_1 n_2}} = 1.8482$$

These satisfy the conditions mentioned in equations (10) and (11).

Transient: The data matrix of size $20(n_1) \times 1200(n_2)$ is considered, which resulted in the following μ values:

$$\mu_0 = \max \{ \mu(U) = 1, \mu(V) = 9.7370 \}$$

These are much smaller as compared to the maximum value of $n/r = 60$. Other values for testing the incoherence property are as follows:

$$\mu_0 = 9.7370, \quad \mu_1 = 43.5451, \quad \max_i \|U^* e_i\|^2 = 1, \\ \max_i \|V^* e_i\|^2 = 0.1623, \quad \|UV^*\|_\infty = 0.2212, \quad \mu_1 \sqrt{\frac{r}{n_1 n_2}} = 1.2570$$

These satisfy the conditions mentioned in equations (10) and (11).

REFERENCES

- [1] A. G. Phadke, “The Wide World of Wide-area measurement,” *IEEE Power and Energy Magazine*, vol. 6, no. 5, pp. 52–65, Sept. 2008.
- [2] Y. Li, D. Yang, F. Liu, Y. Cao, and C. Rehtanz, “Design and implementation of delay-dependent wide-area damping control for stability enhancement of power systems,” in *Interconnected Power Systems*. Springer, 2016, pp. 179–202.
- [3] Y. Cao, X. Shi, Y. Li, Y. Tan, M. Shahidehpour, and S. Shi, “A simplified co-simulation model to investigate impacts of cyber-contingency on power system,” *IEEE Transactions on Smart Grid*, 2017.
- [4] B. Chaudhuri, R. Majumder, and B. C. Pal, “Wide-area measurement-based stabilizing control of power system considering signal transmission delay,” *IEEE Transactions on Power Systems*, vol. 19, no. 4, pp. 1971–1979, 2004.

[5] X. Xie, J. Xiao, C. Lu, and Y. Han, "Wide-area stability control for damping interarea oscillations of interconnected power systems," *IEE Proceedings-Generation, Transmission and Distribution*, vol. 153, no. 5, pp. 507–514, 2006.

[6] M. Zima, M. Larsson, P. Korba, C. Rehtanz, and G. Andersson, "Design aspects for wide-area monitoring and control systems," *Proceedings of the IEEE*, vol. 93, no. 5, pp. 980–996, May 2005.

[7] D. J. Trudnowski, J. W. Pierre, N. Zhou, J. F. Hauer, and M. Parashar, "Performance of three mode-meter block-processing algorithms for automated dynamic stability assessment," *IEEE Transactions on Power Systems*, vol. 23, no. 2, pp. 680–690, 2008.

[8] G. Liu, V. M. Venkatasubramanian, and J. R. Carroll, "Oscillation monitoring system using synchrophasors," in *Power & Energy Society General Meeting, 2009. PES'09. IEEE*. IEEE, 2009, pp. 1–4.

[9] Z. Huang, N. Zhou, F. Tuffner, Y. Chen, D. Trudnowski, W. Mittelstadt, J. Hauer, and J. Dagle, "Improving small signal stability through operating point adjustment," in *Power and Energy Society General Meeting, 2010 IEEE*. IEEE, 2010, pp. 1–8.

[10] Z. Huang, N. Zhou, F. Tuffner, and D. Trudnowski, "Use of modal sensitivity to operating conditions for damping control in power systems," in *System Sciences (HICSS), 2011 44th Hawaii International Conference on*. IEEE, 2011, pp. 1–9.

[11] N. Zhou, D. J. Trudnowski, J. W. Pierre, and W. A. Mittelstadt, "Electromechanical mode online estimation using regularized robust rls methods," *IEEE Transactions on Power Systems*, vol. 23, no. 4, pp. 1670–1680, 2008.

[12] O. Vuković and G. Dán, "Security of Fully Distributed Power System State Estimation: Detection and Mitigation of Data Integrity Attacks," *IEEE J. on Selected Areas in Communications*, vol. 32, no. 7, pp. 1500–1508, Jul. 2014.

[13] S. Cui, Z. Han, S. Kar, T. T. Kim, H. V. Poor, and A. Tajer, "Coordinated Data-injection attack and Detection in the Smart Grid: A Detailed look at enriching Detection Solutions," *IEEE Signal Processing Magazine*, vol. 29, no. 5, pp. 106–115, Sept. 2012.

[14] Y. Liu, P. Ning, and M. K. Reiter, "False Data Injection Attacks Against State Estimation in Electric Power Grids," in *Proc. of the 16th ACM Conference on Computer and Communications Security*, ser. CCS '09, Nov. 2009, pp. 21–32.

[15] A. Tajer, "Energy grid state estimation under random and structured bad data," in *2014 IEEE 8th Sensor Array and Multichannel Signal Processing Workshop (SAM)*. IEEE, 2014, pp. 65–68.

[16] Z.-H. Yu and W.-L. Chin, "Blind false data injection attack using pca approximation method in smart grid," *IEEE Transactions on Smart Grid*, vol. 6, no. 3, pp. 1219–1226, 2015.

[17] A. S. Dobakhshari and A. M. Ranjbar, "A wide-area scheme for power system fault location incorporating bad data detection," *IEEE Transactions on Power Delivery*, vol. 30, no. 2, pp. 800–808, April 2015.

[18] Z. H. Yu and W. L. Chin, "Blind false data injection attack using pca approximation method in smart grid," *IEEE Transactions on Smart Grid*, vol. 6, no. 3, pp. 1219–1226, May 2015.

[19] D. Shi, D. Tylavsky, and N. Logic, "An adaptive method for detection and correction of errors in pmu measurements," in *2013 IEEE Power Energy Society General Meeting*, July 2013, pp. 1–1.

[20] I. Esnaola, S. M. Perlaza, H. V. Poor, and O. Kosut, "Maximum distortion attacks in electricity grids," *IEEE Transactions on Smart Grid*, vol. 7, no. 4, pp. 2007–2015, July 2016.

[21] A. Tajer, "Energy grid state estimation under random and structured bad data," in *2014 IEEE 8th Sensor Array and Multichannel Signal Processing Workshop (SAM)*, June 2014, pp. 65–68.

[22] J. Zhao, G. Zhang, K. Das, G. N. Korres, N. M. Manousakis, A. K. Sinha, and Z. He, "Power system real-time monitoring by using pmu-based robust state estimation method," *IEEE Transactions on Smart Grid*, vol. 7, no. 1, pp. 300–309, Jan 2016.

[23] K. Nishiya, J. Hasegawa, and T. Koike, "Dynamic state estimation including anomaly detection and identification for power systems," *IEE Proceedings C - Generation, Transmission and Distribution*, vol. 129, no. 5, pp. 192–198, September 1982.

[24] A. M. L. da Silva, M. B. D. C. Filho, and J. M. C. Cantera, "An efficient dynamic state estimation algorithm including bad data processing," *IEEE Power Engineering Review*, vol. PER-7, no. 11, pp. 49–49, Nov 1987.

[25] O. Kosut, L. Jia, R. J. Thomas, and L. Tong, "Limiting false data attacks on power system state estimation," in *2010 44th Annual Conference on Information Sciences and Systems (CISS)*, March 2010, pp. 1–6.

[26] A. T. H. Sandberg and K. H. Johansson, "On security indices for state estimators in power networks," in *1st Workshop Secure Control Syst., Stockholm, Sweden*, 2010.

[27] R. J. T. O. Kosut, L. Jia and L. Tong, "Malicious data attacks on smart grid state estimation: Attack strategies and countermeasures," in *1st IEEE Int. Conf. Smart Grid Commun., Gaithersburg, MD, USA*, 2010, p. 220–225.

[28] A. Teixeira, S. Amin, H. Sandberg, K. H. Johansson, and S. S. Sastry, "Cyber security analysis of state estimators in electric power systems," in *49th IEEE Conference on Decision and Control (CDC)*, Dec 2010, pp. 5991–5998.

[29] S. Pan, T. Morris, and U. Adhikari, "Classification of disturbances and cyber-attacks in power systems using heterogeneous time-synchronized data," *IEEE Transactions on Industrial Informatics*, vol. 11, no. 3, pp. 650–662, June 2015.

[30] —, "Developing a hybrid intrusion detection system using data mining for power systems," *IEEE Transactions on Smart Grid*, vol. 6, no. 6, pp. 3104–3113, Nov 2015.

[31] H. M. Khalid and J. C. H. Peng, "A bayesian algorithm to enhance the resilience of wams applications against cyber attacks," *IEEE Transactions on Smart Grid*, vol. 7, no. 4, pp. 2026–2037, July 2016.

[32] Z. Zhou, X. Li, J. Wright, E. Candes, and Y. Ma, "Stable principal component pursuit," in *Information Theory Proceedings (ISIT), 2010 IEEE International Symposium on*. IEEE, 2010, pp. 1518–1522.

[33] E. J. Candès, X. Li, Y. Ma, and J. Wright, "Robust principal component analysis?" *Journal of the ACM (JACM)*, vol. 58, no. 3, p. 11, 2011.

[34] E. Candes and B. Recht, "Exact matrix completion via convex optimization," *Communications of the ACM*, vol. 55, no. 6, pp. 111–119, 2012.

[35] Z. Lin, M. Chen, and Y. Ma, "The augmented lagrange multiplier method for exact recovery of corrupted low-rank matrices," *arXiv preprint arXiv:1009.5055*, 2010.

[36] X. Yuan and J. Yang, "Sparse and low-rank matrix decomposition via alternating direction methods," *preprint*, vol. 12, 2009.

[37] K. Mahapatra, N. R. Chaudhuri, and R. Kavasseri, "Bad data detection in pmu measurements using principal component analysis," in *North American Power Symposium (NAPS)*, 2016. IEEE, 2016, pp. 1–6.

[38] I. Kamwa, R. Grondin, E. J. Dickinson, and S. Fortin, "A minimal realization approach to reduced-order modelling and modal analysis for power system response signals," *IEEE Transactions on Power Systems*, vol. 8, no. 3, pp. 1020–1029, 1993.

[39] J. J. Sanchez-Gasca and J. H. Chow, "Performance comparison of three identification methods for the analysis of electromechanical oscillations," *IEEE Transactions on Power Systems*, vol. 14, no. 3, pp. 995–1002, 1999.

[40] R. W. Wies, J. W. Pierre, and D. J. Trudnowski, "Use of arma block processing for estimating stationary low-frequency electromechanical modes of power systems," *IEEE Power Engineering Review*, vol. 22, no. 11, pp. 57–57, 2002.

[41] N. Zhou, J. W. Pierre, D. J. Trudnowski, and R. T. Guttrumson, "Robust rls methods for online estimation of power system electromechanical modes," *IEEE Transactions on Power Systems*, vol. 22, no. 3, pp. 1240–1249, 2007.

[42] L. Ljung, *System identification: theory for the user*, 2nd ed. Upper Saddle River, N.J.: Prentice Hall PTR; London : Prentice-Hall International, 1999.

[43] C. Eckart and G. Young, "The approximation of one matrix by another of lower rank," *Psychometrika*, vol. 1, no. 3, pp. 211–218, 1936.

[44] I. T. Jolliffe, "Principal component analysis. series in statistics," 1986.

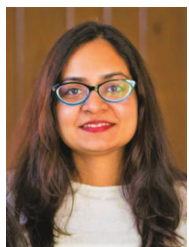
[45] M. Hornstein, "Conditions for robust principal component analysis," *Rose-Hulman Undergraduate Mathematics Journal*, vol. 12, no. 2, p. 9, 2011.

[46] Z. Lin, A. Ganesh, J. Wright, L. Wu, M. Chen, and Y. Ma, "Fast convex optimization algorithms for exact recovery of a corrupted low-rank matrix," *Computational Advances in Multi-Sensor Adaptive Processing (CAMSAP)*, vol. 61, no. 6, 2009.

[47] J. Wright, A. Ganesh, S. Rao, Y. Peng, and Y. Ma, "Robust principal component analysis: Exact recovery of corrupted low-rank matrices via convex optimization," in *Advances in neural information processing systems*, 2009, pp. 2080–2088.

[48] D. P. Bertsekas, *Constrained optimization and Lagrange multiplier methods*. Academic press, 2014.

[49] B. Pal and B. Chaudhuri, *Robust control in power systems*, ser. Power electronics and power systems. New York: Springer, 2005.



Kaveri Mahapatra (S'16) received the M. Tech. degree from Siksha 'O' Anusandhan University, India in 2013. She is currently pursuing her Ph.D. degree in the School of Electrical Engineering and Computer Science at the Pennsylvania State University, USA. Her current research interests include wide-area monitoring, protection and control, cybersecurity, soft computing and optimization, and power system dynamics.



Nilanjan Ray Chaudhuri (S'08-M'09-SM'16) received his Ph.D. degree from Imperial College London, London, UK in 2011 in Power Systems. From 2005-2007, he worked in General Electric (GE) John F. Welch Technology Center. He came back to GE and worked in GE Global Research Center, NY, USA as a Lead Engineer during 2011-2014. Presently, he is an Assistant Professor with the School of Electrical Engineering and Computer Science at Penn State, University Park, PA. He was an Assistant Professor with North Dakota State University, Fargo, ND, USA during 2014-2016. He is a member of the *IEEE* and *IEEE PES*. Dr. Ray Chaudhuri is the lead author of the book *Multi-terminal Direct Current Grids: Modeling, Analysis, and Control* (Wiley/IEEE Press, 2014), and an Associate Editor of the *IEEE TRANSACTIONS ON POWER DELIVERY*. Dr. Ray Chaudhuri is the recipient of the National Science Foundation Early Faculty CAREER Award in 2016.